REPORT DOCUMENTATION PAGE

Form Approved OMB NO. 0704-0188

1. REPORT DATE (DD-MM-YYYY)	2. REPORT TYPE	3. DATES COVERED (From - To)
12-12-2008	New Reprint	1-Jul-2007 - 21-May-2008

4. TITLE AND SUBTITLE

Sound-wave coherence in atmospheric turbulence with intrinsic and global intermittencya)

5a. CONTRACT NUMBER
W911NF-06-1-0007

5b. GRANT NUMBER

5c. PROGRAM ELEMENT NUMBER
206022

6. AUTHORS

D. K. Wilson, V. E. Ostashev, G. H. Goedecke

5d. PROJECT NUMBER

5e. TASK NUMBER

5f. WORK UNIT NUMBER

7. PERFORMING ORGANIZATION NAMES AND ADDRESSES

New Mexico State University
1620 Standley Drive
Academic Research Bldg A, Room 110
Las Cruces, NM 88003 -

8. PERFORMING ORGANIZATION REPORT NUMBER

9. SPONSORING/MONITORING AGENCY NAME(S) AND ADDRESS(ES)

U.S. Army Research Office
P.O. Box 12211
Research Triangle Park, NC 27709-2211

10. SPONSOR/MONITOR'S ACRONYM(S)
ARO

11. SPONSOR/MONITOR'S REPORT NUMBER(S)
49504-EV-HSI.11

12. DISTRIBUTION AVAILIBILITY STATEMENT

Approved for Public Release; Distribution Unlimited

13. SUPPLEMENTARY NOTES

The views, opinions and/or findings contained in this report are those of the author(s) and should not contrued as an official Department of the Army position, policy or decision, unless so designated by other documentation.

14. ABSTRACT

The coherence function of sound waves propagating through an intermittently turbulent atmosphere is calculated theoretically. Intermittency mechanisms due to both the turbulent energy cascade (intrinsic intermittency) and spatially uneven production (global intermittency) are modeled using ensembles of quasiwavelets (QWs), which are analogous to turbulent eddies. The intrinsic
intermittency is associated with decreasing spatial density (packing fraction) of the QWs with decreasing size. Global intermittency is introduced by allowing the local strength of the turbulence, as manifested by the amplitudes of the QWs, to

15. SUBJECT TERMS

atmospheric turbulence, global and intrinsic intermittency

16. SECURITY CLASSIFICATION OF:			17. LIMITATION OF ABSTRACT	15. NUMBER OF PAGES	19a. NAME OF RESPONSIBLE PERSON
a. REPORT	b. ABSTRACT	c. THIS PAGE			Vladimir Ostashev
U	U	U	SAR		19b. TELEPHONE NUMBER 505-646-3832

Report Title

Sound-wave coherence in atmospheric turbulence with intrinsic and global intermittencya)

ABSTRACT

The coherence function of sound waves propagating through an intermittently turbulent atmosphere is calculated theoretically. Intermittency mechanisms due to both the turbulent energy cascade (intrinsic intermittency) and spatially uneven production (global intermittency) are modeled using ensembles of quasiwavelets (QWs), which are analogous to turbulent eddies. The intrinsic intermittency is associated with decreasing spatial density (packing fraction) of the QWs with decreasing size. Global intermittency is introduced by allowing the local strength of the turbulence, as manifested by the amplitudes of the QWs, to vary in space according to superimposed Markov processes. The resulting turbulence spectrum is then used to evaluate the coherence function of a plane sound wave undergoing line-of-sight propagation. Predictions are made by a general simulation method and by an analytical derivation valid in the limit of Gaussian fluctuations in signal phase. It is shown that the average coherence function increases as a result of both intrinsic and global intermittency. When global intermittency is very strong, signal phase fluctuations become highly non-Gaussian and the average coherence is dominated by episodes with weak turbulence.

Sound-wave coherence in atmospheric turbulence with intrinsic and global intermittency[a)]

D. Keith Wilson[b)]
U.S. Army Engineer Research and Development Center, 72 Lyme Road, Hanover, New Hampshire 03755

Vladimir E. Ostashev[c)]
NOAA/Earth System Research Laboratory, Boulder, Colorado 80303 and Physics Department, New Mexico State University, Las Cruces, New Mexico 88003

George H. Goedecke[d)]
Physics Department, New Mexico State University, Las Cruces, New Mexico 88003

(Received 28 January 2008; revised 21 May 2008; accepted 21 May 2008)

The coherence function of sound waves propagating through an intermittently turbulent atmosphere is calculated theoretically. Intermittency mechanisms due to both the turbulent energy cascade (intrinsic intermittency) and spatially uneven production (global intermittency) are modeled using ensembles of quasiwavelets (QWs), which are analogous to turbulent eddies. The intrinsic intermittency is associated with decreasing spatial density (packing fraction) of the QWs with decreasing size. Global intermittency is introduced by allowing the local strength of the turbulence, as manifested by the amplitudes of the QWs, to vary in space according to superimposed Markov processes. The resulting turbulence spectrum is then used to evaluate the coherence function of a plane sound wave undergoing line-of-sight propagation. Predictions are made by a general simulation method and by an analytical derivation valid in the limit of Gaussian fluctuations in signal phase. It is shown that the average coherence function increases as a result of both intrinsic and global intermittency. When global intermittency is very strong, signal phase fluctuations become highly non-Gaussian and the average coherence is dominated by episodes with weak turbulence.
 [DOI: 10.1121/1.2945162]

PACS number(s): 43.28.Gq, 43.20.Fn, 43.28.Lv [RMW] Pages: 743–757

I. INTRODUCTION

The main purpose of this article is to examine how turbulent intermittency affects the coherence of propagating sound waves. Coherence of sound in a turbulent atmosphere is important for remote sensing [1] and assessment of performance of acoustic arrays for source localization.[2] Theoretical treatments of the coherence function (which describes the dependence of coherence on spatial separation between the observation points) for waves propagating in a random medium are well developed in many regards.[3–6] The calculated coherence function depends significantly on the model for the turbulence. In recent years, turbulence models have become more realistic in contrast to early studies that dealt with homogeneous, isotropic random scalar fields possessing a Gaussian correlation function. For example, the coherence function has now been calculated for the case of inhomogeneous, anisotropic turbulence with realistic spectra of temperature and wind velocity fluctuations.[7,8] Here, we consider the introduction of an additional realism, namely, intermittency.

Intermittency refers to the tendency of turbulence to occur in spatial and temporal bursts of activity. This property of turbulence[9,10] plays an important role in many practical problems. Mahrt[11] has proposed classifying intermittency as *intrinsic* or *global*. The former occurs on scales less than the outer scale of turbulence (the scale of largest eddies) as the turbulent cascade process progressively concentrates turbulent energy dissipation into smaller regions of space.[12] Global intermittency occurs on scales larger than the outer scale and may have several causes related to uneven production of turbulence in a particular environment. Possible causes include wind gusts from large-scale convective systems or topographic flow, irregular episodes of turbulent mixing in stably stratified (night time) boundary layers, large organized coherent structures, and uneven heating of the ground due to clouds and variations in ground-surface properties. The terms *small scale* and *large scale* are also used to describe intrinsic and global intermittency, respectively. [11,13]

Figure 1 is a conceptual illustration of intermittency and its effects on wave propagation. The eddies occur in "clouds," each of which represents a global intermittency event. Each turbulent cloud can be regarded as having its own outer scale and turbulent strength. Within each cloud, the smaller eddies organize into intermittent patches as a result of the turbulent cascade process (intrinsic intermittency). The scattering experienced by sound waves propagating along various paths through this region varies greatly,

[a)]Portions of this work were presented in V. E. Ostashev, D. K. Wilson, and G. H. Goedecke "Intermittent scalar QW model and sound propagation through intermittent turbulence," in *Proceedings of the 12th Long Range Sound Propagation Symposium*, New Orleans, LA, 2006, pp. 429–442.
[b)]Electronic mail: d.keith.wilson@usace.army.mil
[c)]Electronic mail: vladimir.ostashev@noaa.gov
[d)]Electronic mail: ggoedeck@nmsu.edu

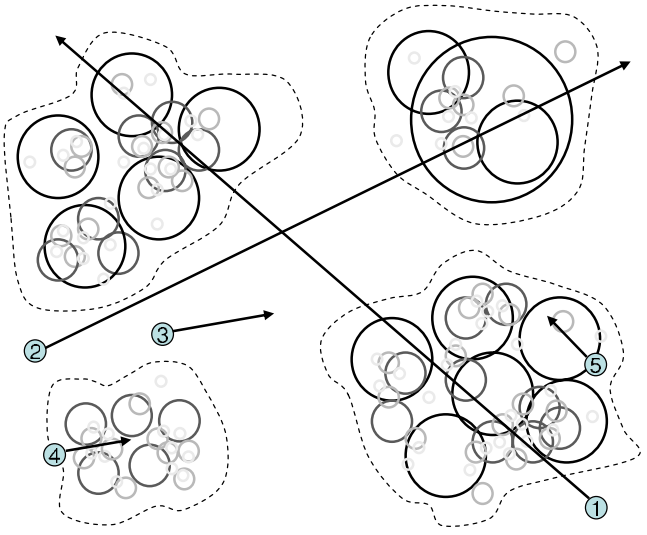

FIG. 1. (Color online) Illustration of intrinsic and global intermittency, and their effects on wave propagation. The solid circles represent turbulent eddies and the dashed lines represent global regions of active turbulence. The numbers and arrows indicate illustrative propagation paths as described in the text.

according to the number and intensity of clouds encountered. Propagation paths that are longer than or comparable to the size of the clouds, such as paths 1 and 2, experience regions of weak and strong turbulence due to global, and to a lesser extent due to intrinsic, intermittency. Paths 3–5 are short compared to the size of the clouds and therefore experience either strong or weak globally intermittent patches. Since path 3 does not actually pass through a cloud, sound waves propagating along this path experience very little scattering. Paths 4 and 5 are through similar globally strong regions, but scattering is stronger along path 4 because of differences in intrinsic intermittency.

Several previous studies have dealt with the effect of intrinsic intermittency on electromagnetic[14,15] and acoustic[16–19] propagation. The underlying idea of these studies is that if the propagating waves sample a region smaller than the outer scale, the index-of-refraction structure-function parameter C_n^2 for the scattering region (which describes the strength of the inertial-subrange spectrum in this region) becomes a random variable. The statistics of the varying C_n^2 can be described by the well-known log-normal model.[20] According to this model, the smaller the sample region, the greater the fluctuations in C_n^2.

Other studies have explicitly considered global intermittency effects on wave propagation, or provide treatments for intermittency effects that are not specifically global or intrinsic.[21–27] In these studies, it is generally assumed that the length of the propagation path is large compared to the outer scale. Hence, the fluctuations in C_n^2 resulting from intrinsic intermittency are unimportant. However, statistical parameters for the turbulence, including C_n^2, may still vary as a result of globally intermittent processes. Hentschel and Procaccia[22] considered an effect of intrinsic intermittency, namely, the modification of the well-known $-11/3$ power law for inertial-subrange turbulence, over global-scale propagation paths. Petenko and Shurygin[27] combined a two-regime model for global intermittency with a log-normal model for intrinsic intermittency.

In comparison to previous works, in this article we study the effects of combined intrinsic and global intermittency on coherence for line-of-sight, plane-wave sound propagation through a turbulent atmosphere. Of course, in order to model the propagation in intermittent turbulence, one must first model the intermittency. A sizable portion of the article is concerned with a quasiwavelet (QW) model of intermittency. A QW is a localized perturbation, analogous to a turbulent eddy, to the temperature and/or velocity field.[28,29] Several QW models of atmospheric turbulence have been developed recently, in which turbulence is represented as a collection of self-similar QWs of many different sizes.[28,30–32] These and similar models have been used for studies of wave propagation and scattering in a turbulent atmosphere.[33–37] Due to their spatially localized nature, QWs can be a useful tool for describing turbulence and other random phenomena with intrinsic and global intermittency features. QWs are also especially well suited to modeling inhomogeneous, anisotropic turbulence because, unlike customary wavelets, they may be distributed and oriented nonuniformly in space according to any desired joint probability distributions.

In this paper, we first obtain formulas for the three-dimensional (3D) spectrum, correlation function, variance, and kurtosis predicted by a QW model of temperature fluctuations with intrinsic intermittency. Then, the QW model is generalized to account for global intermittency. Although both temperature and velocity fluctuations affect the coherence of a sound wave propagating in a turbulent atmosphere, their contributions are additive and hence can reasonably be studied separately.[6,28,30] We therefore simplify the development of a QW model of turbulence with intrinsic and global intermittency by considering only temperature fluctuations. Reference 32 reports on preliminary results in developing a QW model of intermittent velocity fluctuations. Also, although we apply the model here to sound-wave propagation through turbulence, it potentially has broader applications, e.g., to electromagnetic propagation, geological heterogeneities close to Earth's surface and within the Earth,[38] boundary-layer meteorology, and eddy-based simulation of turbulence.

This paper is organized as follows. In Sec. II, a QW model of temperature fluctuations with intrinsic intermittency is developed. The model is generalized in Sec. III to include global intermittency along a one-dimensional path. In Sec. IV, this statistical framework for describing intrinsic and global intermittency is used as the basis for a theory of the coherence function of a sound wave propagating in a turbulent atmosphere. Predictions of the theory are studied with numerical simulation methods, and analytical approximations are derived and compared to the simulations. In Sec. V, the obtained results are summarized.

II. QW MODEL FOR INTERMITTENT SCALAR FLUCTUATIONS

In this section, basic formulas describing a QW model for fluctuations in scalar quantities are briefly discussed.

(The reader may refer to articles cited in the Introduction for more details.) Then, these formulas are used to develop QW models of temperature fluctuations with intrinsic and global intermittency.

A. Basic formulas

The underlying idea of the QW model is to represent a random field as a collection of randomly placed and oriented objects. The objects, like customary wavelets, are spatially localized and based on rescaling and translation of a parent function. However, some properties of customary wavelets, such as zero mean, can be relaxed. Their sizes and amplitudes can be selected according to any desired scaling laws. Lovejoy and Mandelbrot[39] have called this sort of self-similar representation a "fractal sum of pulses." Although most of the discussion to follow explicitly deals with turbulent temperature fields, the same modeling approach can be applied to other types of scalar fluctuations. For a QW model of turbulence, the individual QWs are roughly analogous to turbulent eddies.

A single temperature QW is a perturbation $\Delta T^{\alpha n}(\mathbf{R})$ to the mean field given by

$$\Delta T^{\alpha n}(\mathbf{R}) = \tau^{\alpha n}\Delta T_\alpha f(|\mathbf{R}-\mathbf{b}^{\alpha n}|/a_\alpha). \tag{1}$$

Here, $\mathbf{R}=(x,y,z)$ are the Cartesian coordinates, and $\alpha=1,2,\ldots,N$ and $n=1,2,\ldots,N_\alpha$ are two indices, which determine a particular QW. The index α determines the size a_α of a QW: There are N QW sizes arranged in a diminishing order: $a_1>a_2>\cdots>a_N$. The largest a_1 and smallest a_N sizes are of the order of outer and inner scales of turbulence. In a QW model, there are N_α QWs with the same size a_α; individual QWs in a size class are distinguished by the index n. Furthermore, in Eq. (1) $\mathbf{b}^{\alpha n}$ are the coordinates of the center of the αnth QW, ΔT_α is its amplitude, $\tau^{\alpha n}$ is a random sign factor with zero mean and unit variance,[40] and f is the parent function describing the shape of the QW. Note that $\mathbf{b}^{\alpha n}$ is a random vector within the volume V where turbulence is modeled and f is the same for all QWs. Different parent functions f can be used in QW models. In what follows, a theoretical development will be done for an arbitrary parent function f. Specific results will subsequently be obtained for the Gaussian parent function, given by $f(\chi)=(2\pi)^{3/2}\exp(-\chi^2/2)$, where χ is a nondimensional argument. The overall field of temperature fluctuations $\tilde{T}(\mathbf{R})$ is the sum of contributions from the individual QWs as follows:

$$\tilde{T}(\mathbf{R}) = \sum_{\alpha=1}^{N}\sum_{n=1}^{N_\alpha}\Delta T^{\alpha n}(\mathbf{R}). \tag{2}$$

Here, the sums are taken over all QW sizes used and over all QWs within a particular size class.

A correlation function $B(\mathbf{R})$ of temperature fluctuations is defined as follows:

$$B(\mathbf{R}_1-\mathbf{R}_2) = \langle\tilde{T}(\mathbf{R}_1)\tilde{T}(\mathbf{R}_2)\rangle, \tag{3}$$

where the brackets $\langle\ \rangle$ denote ensemble average and it is assumed that temperature fluctuations are statistically homogeneous. The 3D spectrum $\Phi(\kappa)$ of temperature fluctuations, where κ is the turbulence wave vector, is a Fourier transform of $B(\mathbf{R})$. For the case of isotropic, homogeneous turbulence, $\Phi(\kappa)$ depends only on the magnitude of the vector κ. Substituting Eqs. (1) and (2) into Eq. (3), and assuming that the $\mathbf{b}^{\alpha n}$ and $\tau^{\alpha n}$ are mutually independent, the following formula for $\Phi(\kappa)$ can be obtained by averaging over an ensemble of random realizations:[30]

$$\Phi(\kappa) = 8\pi^3\sum_{\alpha=1}^{N}\phi_\alpha a_\alpha^3\Delta T_\alpha^2 F^2(\kappa a_\alpha). \tag{4}$$

Here, $\phi_\alpha=N_\alpha a_\alpha^3/V$ is the packing fraction of the QWs with the same size a_α, which is proportional to the ratio of the volume occupied by these QWs to the total volume $\mathcal{V}$ where temperature fluctuations are simulated. Furthermore, in Eq. (4) $F(\xi)$ is the spectral parent function; that is, the Fourier transform of the parent function $f(\chi)$. For the Gaussian parent function, $F(\xi)=\exp(-\xi^2/2)$.

The correlation function $B(R)$ is the inverse Fourier transform of $\Phi(\kappa)$. By the convolution theorem, the inverse transform of $F^2(\xi)$ is the convolution of $f(\chi)$ with itself. Hence, the correlation function is

$$B(R) = \sum_{\alpha=1}^{N}\phi_\alpha\Delta T_\alpha^2 f_2(R/a_\alpha), \tag{5}$$

where $f_2(\chi)$ is defined as

$$f_2(\chi) = f(\chi) * f(\chi) = \int d^3\chi' f(|\chi-\chi'|)f(\chi'). \tag{6}$$

The preceding formulas are quite general and can be used to model random fields having a range of properties. To capture the properties of turbulence, certain scaling relationships should be imposed on the QW sizes a_α, the packing fractions ϕ_α, and the temperature amplitudes ΔT_α. For example, to model statistically isotropic, homogeneous, and nonintermittent temperature fluctuations, the scaling relationships can be chosen as follows:[30]

$$a_\alpha = a_1 e^{-\mu(\alpha-1)}, \quad \phi_\alpha = \text{const}, \quad \Delta T_\alpha = \Delta T_1(a_\alpha/a_1)^{1/3}, \tag{7}$$

where μ is a positive parameter usually much smaller than 1. According to the first of these scaling relationships, the neighboring sizes have a constant ratio $(e^{-\mu})$, which mimics a self-similar turbulent cascade of eddies with different sizes. The second relationship in Eq. (7) ensures that QWs with different sizes occupy the same total volume, which is expected for nonintermittent turbulence. Finally, the third relationship produces the classical Kolmogorov spectrum of temperature fluctuations in the inertial subrange as should be the case for isotropic, homogeneous turbulence. After substitution of Eq. (7) into Eq. (4) and some algebra, a spectrum $\Phi(\kappa)$ qualitatively similar to von Kármán's is obtained.[30]

Figure 2(a) shows an example, random QW field. This realization was made from 362 size classes ranging from $a_N=0.2$ m to $a_1=10$ m. (QWs smaller than 0.2 m would not be apparent in the image.) The packing fraction ϕ is 0.0023 for all size classes and $\Delta T_1=0.5$ K. The QWs are distributed

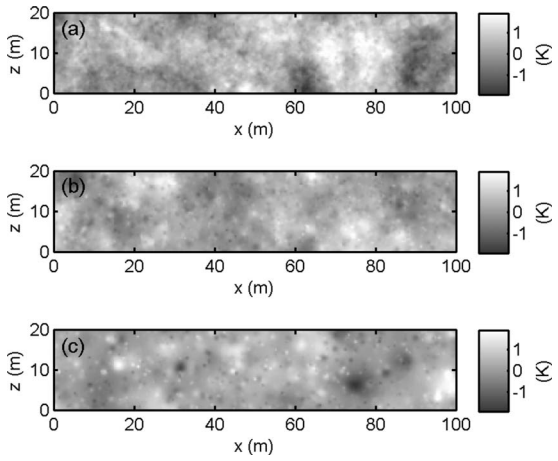

FIG. 2. Examples of synthetic turbulence fields produced by random QW ensembles. (a) Example without intermittency. (b) Example with intrinsic intermittency ($\lambda=0.5$). (c) Same as (b), except that the packing fraction has been multiplied by $1/3$, and the amplitudes by $\sqrt{3}$. All scales are in K.

uniformly in a $160\times60\times80$ m^3 volume. A 100×20 m^2 cross section along the *xz*-plane is shown. To mitigate edge effects, the cross section is centered within the volume such that all displayed points are at least 30 m ($3a_1$) from a side of the volume.

B. Intrinsic intermittency

1. Scaling relationships and cascades

To model temperature fluctuations with intrinsic intermittency, the scaling relationships for a_α, ϕ_α, and ΔT_α must be chosen to capture the main properties of such fluctuations. Regardless of whether intermittency is present, we anticipate that the turbulence is a self-similar cascade process and thus the distribution of size classes continues to be dictated by the first relationship in Eq. (7). However, for turbulence with intrinsic intermittency, small eddies become less and less space filling[12] so that the second relationship in Eq. (7) does not hold. To accommodate this property of intermittent scalar turbulence, we assume (similarly to Ref. 32 where intermittent velocity fluctuations were considered) that the packing fraction ϕ_α decreases as the QW size becomes smaller as follows:

$$\phi_\alpha = \phi(a_\alpha/a_1)^\lambda. \tag{8}$$

Here, ϕ is a constant that is equal to the packing fraction ϕ_1 of the largest QWs and $\lambda\geqslant0$ is a parameter characterizing a degree of intrinsic intermittency. The greater the parameter λ, the more intermittent the turbulence; $\lambda=0$ corresponds to the nonintermittent case.

The cascade mechanism by which the small eddies become less space filling controls the spatial distribution of the QWs. In turbulence literature, the cascade mechanism is often conceived as a process repeated from one "generation" to the next: Parent eddies produce children eddies that are contained within, yet do not entirely fill, the space of the parents. For example, a parent eddy of size a may break down into several eddies of size $a/2$. In three dimensions, 2^3 children eddies would be needed to maintain the packing fraction. Less than 2^3 eddies would decrease the packing fraction. This description coincides to the well-known beta model of Frisch *et al.*,[12] which defines the parameter β as the number of children eddies divided by 2^3. Since $\beta=\phi_{\alpha+1}/\phi_\alpha=(a_{\alpha+1}/a_\alpha)^\lambda$ when $a_{\alpha+1}/a_\alpha=1/2$, it follows that $\beta=2^{-\lambda}$. Frisch *et al.*[12] showed that $\beta=2^{D-3}$, where $D\approx2.5$ is the fractal dimension. Hence, $\lambda=3-D\approx0.5$.

Schmitt *et al.*[41] described a procedure for "scale densification" of the beta model that removes the restriction of the parent eddy size being an integer multiple of the size of the children. Lovejoy and Scherzer generalized the beta model so that regions are not perfectly active or inactive.[42] Conceivably, the beta model or such a generalization thereof could be adapted to place the QWs in space according to a cascade process. However, there are many challenges, such as how to provide a continuous placement of the QWs and how to derive statistical results when the size classes are not independent. Also, the beta model is highly idealized: Actual eddies are swept through space during a cascade process and the cascade process may be at different ages in different regions of space. For present purposes, we do not attempt to formulate a cascade spatial construction with the QWs; the positions of QWs in each size class are independent of each other and of the positions of QWs in the preceding size class. This assumption is actually consistent with the fractal sum of pulses method described by Lovejoy and Mandelbrot.[39]

Intrinsic intermittency of turbulence can also affect the scaling relationship for QW amplitudes ΔT_α. To accommodate this possibility, the scaling relationship for ΔT_α is specified as follows:

$$\Delta T_\alpha = \Delta T_1(a_\alpha/a_1)^{1/3}(\phi/\phi_\alpha)^\eta = \Delta T_1(a_\alpha/a_1)^{1/3-\lambda\eta}, \tag{9}$$

where η is another parameter characterizing the intrinsic intermittency. If $\eta=0$, the scaling relationship described by Eq. (9) coincides with Eq. (7). The value of the parameter η depends on the problem under consideration. For example, the value of η for turbulent temperature fluctuations might differ from that for random heterogeneities within Earth. For turbulence, a value for η can be derived from conservation considerations, as has been previously demonstrated for a QW model of turbulent velocity fluctuations with intrinsic intermittency.[32] Here, we extend this treatment to conservative scalar fluctuations such as temperature.

First, consider the specific (per unit mass) turbulent kinetic energy (TKE). The TKE for size class α is proportional to $\phi_\alpha v_\alpha^2$, where v_α is the characteristic velocity scale. The *rate of transfer* of TKE from eddies with scale a_α to smaller scales should be proportional to the TKE divided by the time scale for the size class, a_α/v_α. Since kinetic energy is neither created nor destroyed within the inertial subrange, the rate of transfer should be invariant for turbulence in equilibrium. Hence, $\phi_\alpha v_\alpha^3/a_\alpha=\phi v_1^3/a_1$ for all α. Substituting with Eq. (8), we then have

$$v_\alpha = v_1(a_\alpha/a_1)^{(1-\lambda)/3}. \tag{10}$$

Similarly, the temperature variance associated with size class α is $\phi_\alpha\Delta T_\alpha^2$. If the rate of variance transfer is to be preserved (as it would be for a conservative scalar in steady turbulence), we must have $\phi_\alpha\Delta T_\alpha^2 v_\alpha/a_\alpha=\phi\Delta T_1^2 v_1/a_1$. Substituting with Eqs. (8) and (9) then yields

$$\Delta T_\alpha = \Delta T_1 (a_\alpha / a_1)^{(1-\lambda)/3} \tag{11}$$

and hence η in Eq. (9) is $1/3$. The value $\eta > 0$ implies that the eddies (QWs) must spin relatively faster, and have a stronger temperature amplitude, to compensate for the decreasing packing fraction.

Figures 2(b) and 2(c) are similar to Fig. 2(a), except that intrinsic intermittency with $\lambda = 0.5$ and $\eta = 1/3$ is included. Figure 2(c) furthermore decreases the packing fraction ϕ by $1/3$ (to 0.000 76) for all size classes while increasing ΔT_1 by $\sqrt{3}$ (to 0.866 K); according to Eq. (4), these rescalings do not alter the spectrum or correlation. With intrinsic intermittency, there are noticeably fewer small QWs, although they are stronger. Decreasing packing fraction also enhances the appearence of intermittency.

2. Spectra and correlations

With these revised scaling relationships, we can now calculate the spectrum $\Phi(\kappa)$ from Eq. (4). In this equation, ϕ_α and ΔT_α are replaced with their values given by Eqs. (8) and (9), respectively, and a_α is replaced with its value given by the first relationship in Eq. (7). In the resulting formula, assuming that $\mu \ll 1$, the sum over α is replaced with the integral over a using Eq. (8) from Ref. 30. As a result, we obtain a formula for the 3D spectrum of temperature fluctuations with intrinsic intermittency as follows:

$$\Phi(\kappa) = C(\kappa a_1)^{-11/3-\nu} \int_{ka_N}^{ka_1} \xi^{8/3+\nu} F^2(\xi) d\xi. \tag{12}$$

Here, the new parameter ν is a combination of the intrinsic intermittency parameters λ and η,

$$\nu \equiv \lambda(1 - 2\eta) \approx 1/6, \tag{13}$$

and the coefficient C is given by

$$C \equiv 8\pi^3 \frac{\phi a_1^3 \Delta T_1^2}{\mu}. \tag{14}$$

Equation (12) describes a 3D spectrum of temperature fluctuations with intrinsic intermittency for an arbitrary parent function $F(\xi)$. If $\nu = 0$, this spectrum coincides with that for nonintermittent temperature fluctuations [Eq. (9) in Ref. 30]. Similarly, from Eq. (5) one finds

$$B(R) = \frac{\phi \Delta T_1^2}{\mu} \left(\frac{R}{a_1} \right)^{2/3+\nu} \int_{R/a_1}^{R/a_N} \chi^{-5/3-\nu} f_2(\chi) d\chi. \tag{15}$$

For the Gaussian spectral parent function $F(\xi) = \exp(-\xi^2/2)$, the integral on the right-hand side of Eq. (12) can then be calculated as

$$\Phi_G(\kappa) = \frac{C}{2} (\kappa a_1)^{-11/3-\nu} [\gamma(11/6 + \nu/2, \kappa^2 a_1^2) - \gamma(11/6 + \nu/2, \kappa^2 a_N^2)]. \tag{16}$$

Here, $\gamma(a,x)$ is the incomplete gamma function and the subscript G stands for "Gaussian." For the case of nonintermittent turbulence, when $\nu = 0$, Eq. (16) coincides with Eq. (11) from Ref. 30 as it should. For sound propagation in a turbulent atmosphere, the sound wavelength is nearly always greater than the inner scale of turbulence, which is of order a_N.

Although Eq. (16) is specific to the Gaussian parent function, results for other reasonable parent functions have a similar dependence on wave number.[28,30] The scaling laws [Eq. (7) for classical turbulence, or Eqs. (8) and (9) for intermittent turbulence], when combined with the fractal size distribution, lead to inertial subranges with a slope independent of the parent function. The choice of parent function is mainly significant in the energy-containing subrange ($\kappa a_1 \ll 1$) and in the transition between subranges.

As for the correlation function, one can show for the Gaussian parent function that

$$f_2(\chi) = 8\pi^{9/2} e^{-\chi^2/4}. \tag{17}$$

One then finds, from Eq. (15),

$$B_G(R) = \frac{\pi^{3/2} C}{2a_1^3} \left(\frac{R}{2a_1} \right)^{2/3+\nu} [\Gamma(-1/3 - \nu/2, R^2/4a_1^2) - \Gamma(-1/3 - \nu/2, R^2/4a_N^2)], \tag{18}$$

where $\Gamma(a,x)$ is the complimentary incomplete gamma function. Since $-1/3 - \nu/2$ is negative for $\nu > -2/3$, and the complete gamma function $\Gamma(a)$ is undefined for a negative argument, it is helpful to apply the recursion formula $\Gamma(a+1,x) = a\Gamma(a,x) + x^a e^{-x}$ to rewrite Eq. (18) as

$$B_G(R) = \frac{\pi^{3/2} C}{(2/3 + \nu) a_1^3} \left[e^{-R^2/4a_1^2} - \left(\frac{R}{2a_1} \right)^{2/3+\nu} \times \Gamma(2/3 - \nu/2, R^2/4a_1^2) - \left(\frac{a_N}{a_1} \right)^{2/3+\nu} e^{-R^2/4a_N^2} + \left(\frac{R}{2a_1} \right)^{2/3+\nu} \Gamma(2/3 - \nu/2, R^2/4a_N^2) \right]. \tag{19}$$

Temperature fluctuations with scale less than a_N often do not affect the coherence function and other statistical moments for line-of-sight sound propagation.[6] Therefore, in Eqs. (16) and (19), it is often reasonable to set $a_N = 0$. The terms involving a_N thus vanish. In the energy subrange of turbulence, where $\kappa a_1 \ll 1$, the incomplete gamma function in Eq. (16) can be approximated as follows: $\gamma(11/6 + \nu/2, \kappa^2 a_1^2) \approx (\kappa a_1)^{11/3+\nu} / (11/6 + \nu/2)$. In this subrange, the 3D spectrum of temperature fluctuations does not depend on κ and is given by $\Phi_G = C/(11/3 + \nu)$. In the inertial subrange, where $\kappa a_1 \gg 1$, the incomplete gamma function in Eq. (16) can be replaced with its asymptotic value for large values of the argument. As a result (with $a_N = 0$), we have

$$\Phi_G(\kappa) = \frac{C\Gamma(11/6 + \nu/2)}{2} (\kappa a_1)^{-11/3-\nu}. \tag{20}$$

It follows from this formula that increasing intermittency (increasing ν) steepens the decay of $\Phi_G(\kappa)$ in the inertial subrange. It is worthwhile to compare $\Phi_G(\kappa)$ given by Eq. (20) with the Kolmogorov spectrum

$$\Phi(\kappa) = AC_T^2\kappa^{-11/3}, \tag{21}$$

which is valid in the inertial subrange of nonintermittent turbulence. Here, $A \simeq 0.033$ is a numerical constant and C_T^2 is the structure-function parameter for temperature fluctuations. For $\nu=0$, Eq. (20) has the same κ-dependence as the classical (nonintermittent) Kolmogorov spectrum. If we constrain the parameters in the QW representation such that

$$Ca_1^{-11/3} = 8\pi^3\frac{\phi\Delta T_1^2}{\mu a_1^{2/3}} = \frac{2A}{\Gamma(11/6+\nu/2)}C_T^2, \tag{22}$$

Eq. (22) implies $\Delta T_1 \sim a_1^{1/3}$. Equation (20) now becomes

$$\Phi_G(\kappa) = AC_T^2\kappa^{-11/3}(ka_1)^{-\nu}. \tag{23}$$

This result is consistent with Eq. 2.20 of Hentschel and Procaccia.[22] In the inertial subrange, the intermittency effect modifies the $\kappa^{-11/3}$ power law to $\kappa^{-11/3-\nu} \approx \kappa^{-23/6}$.

For $R/a_1 \ll 1$, the complementary incomplete gamma function in Eq. (18) can be replaced with the complete gamma function, and one has for the correlation function (neglecting the effect of a_N)

$$B_G(R) \approx \frac{\pi^{3/2}C}{(2/3+\nu)a_1^3}\left[1-\left(\frac{R}{2a_1}\right)^{2/3+\nu}\Gamma(2/3-\nu/2)\right]. \tag{24}$$

The structure function for the field is defined as $D(R) = 2[B(0)-B(R)]$. For small separations, the structure function becomes

$$D_G(R) \approx \frac{\pi^{3/2}C\Gamma(2/3-\nu/2)}{(1/3+\nu/2)a_1^3}\left(\frac{R}{2a_1}\right)^{\nu+2/3}. \tag{25}$$

Substituting with Eq. (22), we have

$$D_G(R) \approx C_T^2R^{2/3}\left(\frac{R}{a_1}\right)^{\nu}, \tag{26}$$

where we have made the definition

$$A = \frac{(1/3+\nu/2)\Gamma(11/6+\nu/2)}{2^{1/3-\nu}\pi^{3/2}\Gamma(2/3-\nu/2)}. \tag{27}$$

(With this definition, $A \simeq 0.033$ when $\nu=0$, as expected.) If a_N is not identically zero, we have for $R \ll a_N$

$$B_G(R) = \frac{\pi^{3/2}C}{2a_1^3}\left(\frac{R}{2a_1}\right)^{\nu+2/3}[\Gamma(-1/3-\nu/2, R^2/4a_1^2) - \Gamma(-1/3-\nu/2, R^2/4a_N^2)]. \tag{28}$$

Using Eq. (20), the 3D spectrum $\Phi_G(\kappa)$ [normalized by $C/(11/3)$, the value of $\Phi_G(0)$ for $\nu=0$] is plotted in Fig. 3 versus the normalized wave parameter κa_1 for $\nu=0$, 0.25, and 0.5. The spectrum $\Phi_G(\kappa)$ has two distinct regions. It is almost constant in the energy subrange, where $\kappa a_1 \ll 1$, and has a power law dependence on κ in the inertial subrange, where $\kappa a_1 \gg 1$. This is consistent with asymptotic behavior of the spectrum in the energy and inertial subranges considered above. Furthermore, it follows from Fig. 3 that the greater the parameter ν, the smaller are the values of the spectrum $\Phi_G(\kappa)$. This tendency is more pronounced in the inertial subrange where the spectral slope steepens with increasing value of this parameter.

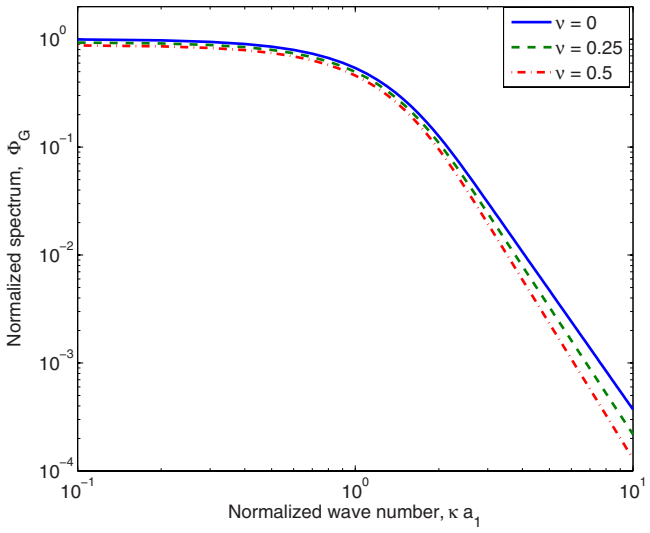

FIG. 3. (Color online) Normalized spectrum Φ_G of intermittent temperature fluctuations vs the normalized wave number κa_1 for different values of the intrinsic intermittency parameter ν.

Figure 4 compares theoretical predictions to the structure function estimated from random realizations of QW fields. The case considered is the same as Fig. 2(b), namely, $a_N=0.2$, $a_1=10$ m, $\phi=0.0023$, and $\Delta T_1=0.5$ K. The estimates were derived from correlation functions of 256 random realizations. The theoretical curves shown are the exact result (with discrete size classes) based on Eq. (5), the continuous size-class approximation based on Eq. (18), and the inertial-subrange approximation, Eq. (25). The simulations and exact result are nearly indistinguishable. For very small separations, the continuous approximation deviates somewhat from the exact result. The inertial-subrange approxima-

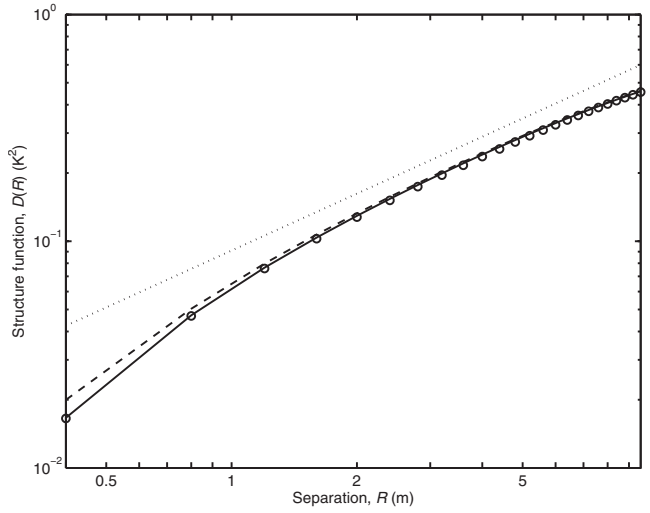

FIG. 4. Structure function for turbulence with intrinsic intermittency. The solid line is an exact curve with discrete spacing between size classes; the dashed line is the corresponding approximation for continuous size classes. The dotted line is an inertial subrange approximation. The circles show the actual structure functions determined from 256 random QW realizations.

tion is seen to be poor for this particular case; apparently, a_N is insufficiently small compared to a_1 for this approximation to be accurate.

3. Variance and kurtosis

The variance of temperature fluctuations σ^2 is needed in many applications. For both intermittent and nonintermittent turbulences, σ^2 can be determined by integrating the 3D spectrum of temperature fluctuations or by taking the limit $R \to 0$ of Eq. (15). Using the latter approach, we have from Eq. (5)

$$\sigma^2 = \sum_{\alpha=1}^{N} \sigma_\alpha^2, \tag{29}$$

where the contribution to the variance from size class α is

$$\sigma_\alpha^2 = \phi_\alpha \Delta T_\alpha^2 f_2(0). \tag{30}$$

To obtain the variance for the intermittent case, ϕ_α and ΔT_α in Eq. (29) are replaced with their values given by Eqs. (8) and (9), respectively. We thus obtain

$$\sigma_\alpha^2 = \phi \Delta T_1^2 (a_\alpha / a_1)^{2/3+\nu}. \tag{31}$$

Setting $a_\alpha = a_1 e^{-\mu(\alpha-1)}$ and recognizing Eq. (29) now as a geometric series, we explicitly determine the sum as

$$\sigma^2 = \phi \Delta T_1^2 f_2(0) \frac{1 - e^{-\mu(2/3+\nu)N}}{1 - e^{-\mu(2/3+\nu)}} \approx \frac{\phi \Delta T_1^2 f_2(0)}{\mu(2/3+\nu)}. \tag{32}$$

The second approximate form is valid when there are many closely spaced size classes ($\mu N \gg 1$ and $\mu \ll 1$). Applying Eqs. (14) and (17) yields the variance for Gaussian QWs as follows:

$$\sigma_G^2 = \frac{\pi^{3/2}}{(2/3+\nu)} \frac{C}{a_1^3}. \tag{33}$$

We see that the variance decreases with increasing intermittency. When $\nu = 1/6$, σ^2 is $4/5$ times its value without intermittency.

The kurtosis K is defined as the normalized fourth moment of a random field, namely, $K = \langle \tilde{T}^4 \rangle / \sigma^4$. Since intermittency generally leads to a kurtosis larger than the value for a Gaussian random variable, namely, $K=3$, determination of the kurtosis is of much interest (e.g., Refs. 43 and 44). A general formula for $\langle \tilde{T}^4 \rangle$ in the QW model is[45]

$$\langle \tilde{T}^4 \rangle = K_t \sum_{\alpha=1}^{N} \phi_\alpha \Delta T_\alpha^4 \Omega + 3 \left(\sum_{\alpha=1}^{N} \sigma_\alpha^2 \right)^2, \tag{34}$$

where $\Omega = \int d^3\xi f^4(\xi)$ and K_t is the fourth moment of the $\tau^{\alpha n}$ (which as described earlier, have a unit variance). For a QW model in which the $\tau^{\alpha n}$ are ± 1 with equal probability, $K_t = 1$. For a model in which the $\tau^{\alpha n}$ are normally distributed, $K_t = 3$. Equation (34) is valid for both intermittent and nonintermittent turbulence. To obtain the value of K for the intermittent case, a_α, ϕ_α, and ΔT_α are replaced with their values given by Eqs. (7)–(9), respectively. We thus obtain

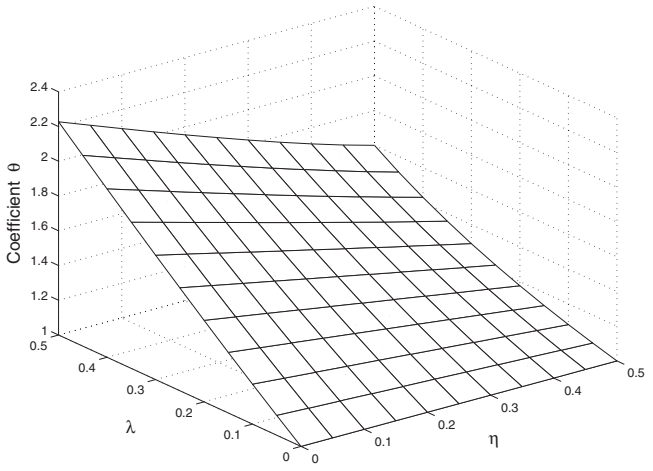

FIG. 5. Coefficient θ, which controls the kurtosis of the QW field, vs the intrinsic intermittency parameters λ and η.

$$K = 3 + \frac{\phi \Delta T_1^4 \Omega K_t}{\sigma^4} \sum_{\alpha=1}^{N} e^{-(\alpha-1)q}, \tag{35}$$

where $q \equiv \lambda(1-4\eta)$. Unlike the variance, the fourth moment [Eq. (34)] is *not* a simple sum of contributions from the size classes. However, Eq. (35) shows that the deviation from Gaussian statistics, $K-3$, can be considered as the sum of contributions from the size classes if the variance is fixed. By calculating the sum in Eq. (35), a formula for the kurtosis of temperature fluctuations with intrinsic intermittency results

$$K = 3 + \frac{\phi \Delta T_1^4 \Omega K_t}{\sigma^4} \frac{1 - e^{-\mu(4/3+q)N}}{1 - e^{-\mu(4/3+q)}} \approx 3 + \frac{\mu(2/3+\nu)^2 \Omega K_t}{\phi(4/3+q)[f_2(0)]^2}. \tag{36}$$

The second, approximate form applies when $\mu N \gg 1$ and $\mu \ll 1$.

The preceding formulas are valid for any parent function. For the Gaussian parent function,[30] $\Omega = (\pi/2)^{3/2}(2\pi)$.[6] Combining this result with Eq. (17), we obtain the kurtosis for the case of the Gaussian parent function

$$K_G = 3 + \frac{\mu \theta K_t}{3(2\pi)^{3/2}\phi}. \tag{37}$$

Here, the coefficient θ is a combination of parameters ν and q (and thus λ and η) as follows:

$$\theta = \frac{(1+3\nu/2)^2}{1+3q/4}. \tag{38}$$

For nonintermittent turbulence, when $\lambda = 0$ and $\theta = 1$, Eq. (37) coincides with Eq. (44) from Ref. 30. The kurtosis can be enhanced either by a low density of QWs (small ϕ/μ) or intrinsic intermittency ($\theta > 1$). Illustrations of the former mechanism can be found in Ref. 30.

In Fig. 5, the coefficient θ is plotted versus the parameters λ and η. It follows from this figure that θ varies in the range from 1 to 2.23 for $0 \leqslant \lambda \leqslant 0.5$ and $0 \leqslant \eta \leqslant 0.5$. Figure 5 can be used in choosing parameters of a QW model of temperature fluctuations leading to a particular value of K_G.

To test the preceding expressions, we compare them to variance and kurtosis from simulations. The cases considered are the same as shown in Fig. 2; results from 256 such random realizations were averaged. For the case without intrinsic intermittency and $\phi=0.0023$, as illustrated in Fig. 2(a), the simulation results (with theoretical values in parentheses) were $\sigma_G^2=0.420$ (0.420) and $K_G=3.41$ (3.34). For the case with intrinsic intermittency and $\phi=0.0023$, as illustrated in Fig. 2(b), the simulation results were $\sigma_G^2=0.343$ (0.350) and $K_G=3.66$ (3.56). For the case with intrinsic intermittency and $\phi=0.000\,76$, as illustrated in Fig. 2(c), the simulation results were $\sigma_G^2=0.350$ (0.350) and $K_G=4.82$ (4.68).

C. Global intermittency

As discussed earlier, global intermittency involves externally imposed variations in turbulence intensity over regions larger than the outer scale of the turbulence. In this section, we consider an approach to incorporating global intermittency into a QW model.

The volume $\mathcal{V}$ where the turbulence is modeled is conceptually subdivided into subvolumes V_i with characteristic scales larger than a_1. Within each of these subvolumes, QWs occur as described in Sec. II B 1, although the parameters may vary from one subvolume to another. In principle, any or all of the parameters ΔT_1, a_1, a_N, ϕ, μ, λ, and η could vary. Variations in the parameters ΔT_1 and a_1 are of particular interest since they depend on the external mechanism creating the turbulence. The inner scale a_N may vary but does not strongly affect sound waves. The ratio ϕ/μ and the parameter λ are expected to have a physical meaning (the packing of QWs as a function of their size) but be fixed for a particular cascade process, such as turbulence. (The individual parameters ϕ and μ are constructive in the QW model but should not vary independently for a particular cascade process.) According to Eq. (14), variations in ΔT_1 and a_1 result in random values of the coefficient C. Then, it follows from Eqs. (22) and (33) that the values of C_T^2 and σ_G^2 are also random and proportional to each other.

To proceed, we need statistical models for the variations in ΔT_1 and/or a_1, or for quantities dependent on them, such as C. Many and varied statistical models for global intermittency have been considered in literature. Mahrt,[11] Petenko and Shurygin,[27] and other authors used dichotomous regions of strong and weak activity. Antonia *et al.*[46] considered a linear ramp model. Tatarskii and Zavorotnyi[21] considered a gamma probability density function (pdf), and Frehlich[24] a log-normal pdf, for C_n^2. This diversity of approaches to modeling global intermittency reflects the different mechanisms producing it as well as the challenges of describing the underlying physics with tractable models.

In the following, we consider a basic model for global intermittency that can be readily related to a QW construction. Depending on how the parameters are adjusted, the model can be made similar to most previous treatments of global intermittency. It involves allowing the quantity C to vary with the coordinate x along a linear path; in our case, this path is the propagation path. The random field $C(x)$ is written as

$$C(x) = \langle C\rangle + C'(x) = \langle C\rangle[1 + \zeta(x)], \tag{39}$$

where $\langle C\rangle$ is the mean value and $C'(x)$ is its fluctuating part, and $\zeta(x)=C'(x)/\langle C\rangle$.

Initially, we consider a two-state Markov process for $C(x)$. (The reader may refer to a text such as Wilks[47] for an introduction to two-state Markov processes.) Within each subvolume V_i along the propagation path, the turbulence is either active (present) or inactive (absent). The inactive state is characterized by $\Delta T_1=0$ and $C=0$; the value for a_1 is thus immaterial. The values of ΔT_1, C, and a_1 are the same for all active subvolumes. Let us designate C_a as the value of C when in the active state, and the actual value of C within V_i as $C_i=C_aX_i$, where X_i is a random variable equal to 0 when V_i is an inactive state and 1 when it is active. The probability of transitioning from an inactive state in the volume V_i to an active state in V_{i+1}, while moving along the propagation path from one subvolume to the next, is designated as p_{01}. The probability of remaining in an active state is designated p_{11}, and so forth. Since there are only two possible outcomes for a transition from a given initial state, we must have $p_{00}+p_{01}=1$ and $p_{10}+p_{11}=1$. This means that only two of the transition probabilities are independent. By convention, these are usually taken to be p_{01} and p_{11}. If the Markov process has positive memory, the probability of transitioning to a particular state is greater if the process is already in that state ($p_{00}>p_{10}$, $p_{11}>p_{01}$). Also of interest are the unconditional probabilities of occurrence for the inactive and active states, designated π_0 and $\pi_1=1-\pi_0$. Since π_1 equals the sum of $p_{01}\pi_0$ and $p_{11}\pi_1$, we have

$$\pi_1 = \frac{p_{01}}{1 + p_{01} - p_{11}}. \tag{40}$$

The following relationships can also be proven:

$$\langle X_i\rangle = \langle X_i^2\rangle = \pi_1, \tag{41}$$

$$\langle X_i'^2\rangle = \langle (X_i - \langle X_i\rangle)^2\rangle = \pi_0\pi_1, \tag{42}$$

$$\langle X'_{i+j}X'_i\rangle = \pi_0\pi_1(p_{11} - p_{01})^j. \tag{43}$$

Statistics involving C_i or C_i' follow after appropriate scaling by C_a, e.g., $\langle C_i\rangle=C_a\pi_1$ and $\langle C_i'^2\rangle=C_a^2\pi_0\pi_1$. Statistics for ζ_i follow from those for X_i' after scaling by π_1^{-1}. Designating the distance between the subvolumes as ℓ, we can write Eq. (43) as

$$\langle X'(x + \Delta x)X'(x)\rangle = \pi_0\pi_1(p_{11} - p_{01})^{|\Delta x|/\ell} = \pi_0\pi_1 e^{-|\Delta x|/L}, \tag{44}$$

where $L=\ell/\ln[1/(p_{11}-p_{01})]$. The transition probabilities can be determined from the mean activity level π_1 and the correlation length by L as follows:

$$p_{01} = \pi_1(1 - e^{-\ell/L}), \quad p_{11} = \pi_1 + \pi_0 e^{-\ell/L}. \tag{45}$$

Next let us suppose $C(x)$ is the average of M independent, identical two-state Markov processes, namely,

$$C(x) = \frac{C_a}{M}\sum_{m=1}^{M} X_i^{(m)}, \tag{46}$$

where each of the $X_i^{(m)}$ follow Eqs. (40)–(43). We then find

$$\langle C(x)\rangle = C_a \pi_1, \tag{47}$$

$$B_C(\Delta x) = \langle C'(x+\Delta x)C'(x)\rangle = \frac{C_a^2 \pi_0 \pi_1}{M} e^{-|\Delta x|/L}, \tag{48}$$

$$B_\zeta(\Delta x) = \langle \zeta(x+\Delta x)\zeta(x)\rangle = \frac{\pi_0}{M\pi_1} e^{-|\Delta x|/L}. \tag{49}$$

Hence, the mean is unaffected, but the variance decreases with increasing M. Since it counts the number of "successful outcomes" of M independent trials with probability π_1, $C(x)$ has a binomial distribution. For large M and π_1 near 0.5, the binomial distribution approaches a Gaussian one. Thus, an advantage of this description for global intermittency is that it encompasses a wide range of behaviors, from two-state (purely active or inactive) to Gaussian.

The local spectrum follows from Eq. (16) but with the random $C(x)$, namely,

$$\Phi_G(x;\kappa) = \frac{C(x)}{2}(\kappa a_1)^{-11/3-\nu}[\gamma(11/6+\nu/2, \kappa^2 a_1^2) - \gamma(11/6+\nu/2, \kappa^2 a_N^2)]. \tag{50}$$

When the contribution from the term involving a_N^2 is negligible, $\kappa a_1 \gg 1$, and intrinsic intermittency is absent ($\nu=0$), our approach reduces to earlier works[21,24] on inertial-subrange intermittency where C_n^2 was allowed to vary with position. Within the volume $\mathcal{V}$, we can calculate the mean spectrum Φ_G by averaging the right-hand side of Eq. (50) over an ensemble of realizations of $C(x)$, which according to Eq. (47) amounts to replacing $C(x)$ with $C_a\pi_1$.

Figure 6 shows two realizations of QW fields with global intermittency. The positions and amplitudes of the QWs are actually the same as Fig. 2(b) (a case with intrinsic intermittency) but are then modulated by a random $C(x)$ process with mean $\langle C(x)\rangle$ matching the original field; hence, the variance of the fields is unchanged. The value of $C(x)$ at the *center position* $\mathbf{b}^{\alpha n}$ is used to tailor its amplitude $\Delta T^{\alpha n}$. Figure 6(a) is a realization of $C(x)/\langle C(x)\rangle$ with $M=1$, $\pi_1=0.25$, and $L=10$ m. The corresponding QW field is shown in Fig. 6(b). This model results in dramatic regions of weak and strong activity. Figure 6(c) is a realization of $C(x)/\langle C(x)\rangle$ with $M=4$, $\pi_1=0.5$, and $L=10$ m. The corresponding QW field is shown in Fig. 6(d). Although the global intermittency is much weaker than Fig. 6(b), there are still pronounced variations in turbulent activity.

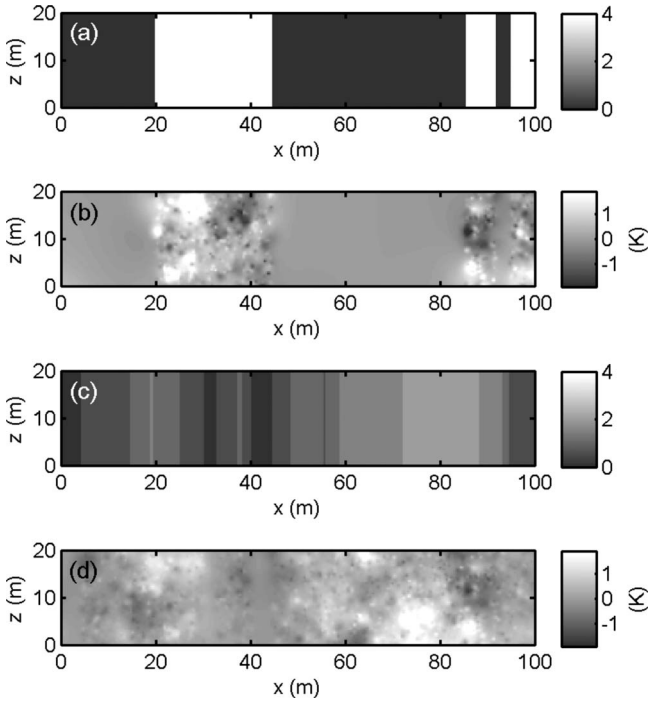

FIG. 6. Examples of synthetic turbulence fields produced by random QW ensembles with global intermittency. (a) Random global intermittency for $C(x)/\langle C\rangle$ produced by a Markov process with $\pi_1=0.25$ and $L=10$ m. (b) Same as the synthetic field in Fig. 2(b), except that the field is modulated by the process in (a). (c) Random global intermittency for $C(x)/\langle C\rangle$ produced by the average of four Markov processes with $\pi_1=0.5$ and $L=10$ m. (d) Same as the synthetic field in Fig. 2(b), except that the field is modulated by the process in (c). Scales for (a) and (c) are dimensionless; scales for (b) and (d) are in K.

III. COHERENCE FUNCTION

In this section, we derive a theory for the coherence of propagating planar sound waves based on the intermittent QW model derived in the previous two sections. The coherence function is defined here as

$$\Gamma(x,r) = \langle p(x,\mathbf{r}_0)p^*(x,\mathbf{r}_0+\mathbf{r})\rangle. \tag{51}$$

Here, $p(x,\mathbf{r})$ is the acoustic pressure, x is the distance from the source plane to the observation plane, and $\mathbf{r}_0$ and $\mathbf{r}_0+\mathbf{r}$ are points in the observation plane. Statistical homogeneity in the observation plane is assumed, so that the coherence is independent of $\mathbf{r}_0$. As mentioned in the Introduction, theories for coherence have already been the subject of much development. Typically, several important assumptions are made: validity of the parabolic approximation, a long propagation path compared to the size of the inhomogeneities, and Gaussian statistics. Intermittency may weaken the validity of the latter two approximations. For example, atmospheric boundary-layer thermals and cloud-driven variations in surface heating, which are sources of intermittency, may extend over several kilometers. In this section, we first consider conceptually how intermittency affects the coherence, and then examine simulation results.

A. Local propagation paths

Initially, let us consider the coherence when the propagation path length x is short compared to the scale L of global intermittency. Paths 3–5 in Fig. 1 illustrate this situation. Intrinsic intermittency, as well as parameter variations induced by global intermittency, can impact on the signal propagation. For example, with the two-state Markov model for global intermittency considered in Sec. II C, the propagation path would be subject to either fully active or inactive

turbulence. This is important because we can consider the statistics of the turbulence to be local and stable over the propagation path.

Previous studies of intermittency have often examined the statistics of point samples and line (or volume) averages of the field. The coherence function actually involves a nonlinear combination of these types of statistics. The interpretation can be made clear for geometric acoustics, in which the sound follows ray paths directly from the source to the receiver. However, interpretation is less clear when diffraction becomes important. In the geometric-acoustics approximation, $p(x,r)=p_0\exp[i\phi(x,r)]$, where $p_0=p$ $(x=0,r)$ for all r, and $\phi(x)$ is a random phase factor given by

$$\phi(x,r)=k\int_0^x n'(x',r)dx'. \tag{52}$$

Here, $n'(x,r)=(c_0/c)-1\approx -c'/c_0$ is a random variation in the index of refraction. (The sound speed is c, c' is its fluctuation, and c_0 its mean.) For temperature fluctuations, which in air are proportional to the squared sound speed, $n'\approx -T'/2T_0$ for temperature fluctuations. Hence, the coherence function is

$$\Gamma(x,r)=p_0^2\left\langle \exp\left[ik\int_0^x [n'(x',0)-n'(x',r)]dx' \right]\right\rangle. \tag{53}$$

This shows that the coherence function for geometric acoustics involves the difference between two line averages separated by a distance r. A nonlinear function (the exponential) of this quantity is then averaged to obtain the coherence. Usually, QWs with size comparable to r will most strongly affect coherence. QWs large compared to r are strong but tend to affect both paths in the same manner, whereas those smaller than r are relatively weaker.

If the phase factors $\phi(x,r)$ are random variables with a Gaussian distribution, the formula $\langle\exp(\varepsilon)\rangle=\exp(\langle\varepsilon^2\rangle/2)$ (where ε is Gaussian with zero mean) leads to

$$\Gamma(x,r)=p_0^2\exp[-D_\phi(x,r)/2], \tag{54}$$

where $D_\phi(x,r)$ is the geometric-acoustics phase structure function, defined as

$$D_\phi(x,r)=\langle[\phi(x,0)-\phi(x,r)]^2\rangle = \frac{k^2}{2T_0^2}\int_0^x\int_0^x [B(x'-x'',0)-B(x'-x'',r)]dx'dx''. \tag{55}$$

When the propagation path is much longer than the size of the inhomogeneities $(x\gg a_1)$,

$$D_\phi(x,r)\approx\frac{k^2x}{2T_0^2}\int_{-\infty}^{\infty}[B(x',0)-B(x',r)]dx'. \tag{56}$$

Using the spectrum, the preceding result can alternatively be written as

$$D_\phi(x,r)\approx\frac{2\pi^2k^2x}{T_0^2}\int_0^\infty \kappa[1-J_0(\kappa r)]\Phi(\kappa)d\kappa. \tag{57}$$

Here, J_0 is the Bessel function of zero order. Hence, we have the following hierarchy: Equation (53) is valid for geometric acoustics, the additional assumption of Gaussian statistics leads to Eqs. (53) and (55), and the further additional assumption of a long propagation path leads to Eqs. (56) and (57). One of the remarkable results of the conventional theory of wave propagation in random media, based on Gaussian statistics and the Markov approximation, is that Eq. (54) with Eq. (57) remains valid in the parabolic approximation even when geometric-acoustics approximations do not. Put another way, when the coherence is calculated with geometric acoustics, the correct general result is obtained, even though the calculation method does not correctly capture the underlying physics involving diffraction or strong scattering. Thus, we may identify limitations to the validity of the conventional theory, such as those stemming from non-Gaussian phase statistics induced by intermittency, by calculating the coherence based on the geometric acoustics. It is plausible that the geometric-acoustics based calculations of the coherence remain correct even when there is intermittency.

Introducing now the complication that C may be a random function (but constant along a particular propagation path), we generalize Eq. (54) as

$$\Gamma_C(x,r)=p_0^2\exp[-D_{\phi,C}(x,r)/2], \tag{58}$$

where $D_{\phi,C}$ and $\Gamma_C(x,r)$ are the structure function and coherence associated with a particular value of C. For the global intermittency model described in Sec. II C, C takes on discrete values C_m following a binomial distribution, so the average coherence function is

$$\overline{\Gamma}(x,r)=\sum_{m=1}^{M}P_m\Gamma_{C_m}(x,r) = p_0^2\sum_{m=1}^{M}P_m\exp[-D_{\phi,C_m}(x,r)/2], \tag{59}$$

where P_m is the probability associated with C_m. If the $D_{\phi,C_m}(x,r)$ are small (i.e., the coherences are high for values of C_m), the approximation $\exp[-D_{\phi,C_m}(x,r)/2]\approx 1-D_{\phi,C_m}(x,r)/2$ leads to the following result:

$$\overline{\Gamma}(x,r)\approx p_0^2\exp[-\overline{D}_\phi(x,r)/2], \tag{60}$$

where

$$\overline{D}_\phi(x,r)=P_mD_{\phi,C_m}(x,r) \tag{61}$$

is the average phase structure function. Since $D_{\phi,C_m}\propto C_m$, $\overline{D}_\phi\propto\langle C\rangle$. However, if the coherence is low and the phase fluctuations are non-Gaussian, we should not expect Eq. (60) to hold.

B. Global propagation paths

We next consider propagation paths that are long compared to the scale L of global intermittency, as illustrated by

paths 1 and 2 in Fig. 1. Such paths involve a varying turbulence spectrum. A treatment for this situation follows from the equation

$$\Gamma(x,r) = p_0^2 \exp\left\{ -\frac{\pi^2 k^2}{T_0^2} \int_0^x dx' \times \int_0^\infty \kappa[1 - J_0(\kappa r)]\Phi(x';\kappa)d\kappa \right\}, \quad (62)$$

which was derived in Ref. 7 for inhomogeneous turbulence. Equation (62) assumes validity of the parabolic equation and the Markov approximation for the random medium, and that the turbulent fluctuations are Gaussian. When the strength of the turbulence varies along the propagation path as described by Eq. (50), we have the following formula for the coherence:

$$\Gamma(x,r) = p_0^2 \exp\left\{ -\frac{k^2}{a_1^2 T_0^2}[W(r/a_1,1) - W(r/a_1,a_N/a_1)] \int_0^x C(x')dx' \right\}, \quad (63)$$

where W is a deterministic function given by

$$W(\rho,s) = \frac{\pi^2}{2} \int_0^\infty \xi^{-8/3-\nu}[1 - J_0(\xi\rho)]\gamma(11/6 + \nu/2, \xi^2 s^2)d\xi. \quad (64)$$

The solution for this integral is given in the Appendix. Note that the right-hand side of Eq. (63) contains a function (the integral) of the random variable $C(x)$. Therefore, to obtain the desired expression for the mean coherence function, both sides of Eq. (63) are averaged over an ensemble of realizations of this integral. (The physical meaning of such averaging is discussed in detail in Ref. 21.) By applying Eq. (39), we can recast Eq. (63) in the following form:

$$\Gamma(x,r) = p_0^2 \exp[-\bar{D}_\phi(x,r)/2] \times \exp\left[-\frac{\bar{D}_\phi(x,r)}{2x} \int_0^x \zeta(x')dx' \right], \quad (65)$$

where

$$\bar{D}_\phi(x,r) = \frac{2\langle C\rangle k^2 x}{a_1^2 T_0^2}[W(r/a_1,1) - W(r/a_1,a_N/a_1)]. \quad (66)$$

The average coherence function is thus

$$\bar{\Gamma}(x,r) = p_0^2 \exp[-\bar{D}_\phi(x,r)/2] \times \left\langle \exp\left[-\frac{\bar{D}_\phi(x,r)}{2x} \int_0^x \zeta(x')dx' \right] \right\rangle. \quad (67)$$

The final part of this expression, with angle brackets, represents the global intermittency effect. It is bounded as follows:

$$1 \leqslant \left\langle \exp\left[-\frac{\bar{D}_\phi(x,r)}{2x} \int_0^x \zeta(x')dx' \right] \right\rangle < \exp[\bar{D}_\phi(x,r)/2]. \quad (68)$$

The first inequality follows from Jensen's inequality, as previously noted in Refs. 21 and 26. The second inequality follows from the argument that $(1/x)\int\zeta(x')dx'$ cannot be smaller than −1, which would correspond to a state of complete inactivity. Thus,

$$1 \geqslant \bar{\Gamma}(x,r)/p_0^2 \geqslant \exp[-\bar{D}_\phi(x,r)/2]. \quad (69)$$

Hence, for a fixed value of $\langle C\rangle$, intermittency always *increases* the average coherence.

According to the global intermittency model in Sec. II C, in some situations $\zeta(x)$ approaches a Gaussian distribution. Actually, since the integral of $\zeta(x)$ is effectively the sum of many samples of $\zeta(x)$ when $x \gg L$, it is even less restrictive to consider the integral as a Gaussian random variable. Assuming this is the case, we obtain the average coherence function

$$\bar{\Gamma}(x,r) = p_0^2 \exp[-\bar{D}_\phi(x,r)/2 + \bar{D}_\phi^2(x,r)I_\zeta/8x^2], \quad (70)$$

where I_ζ is the following integral:

$$I_\zeta = \int_0^x \int_0^x B_\zeta(x_1 - x_2)dx_1 dx_2 = 2\sigma_\zeta^2 Lx\left[1 - \frac{L}{x}(1 - e^{-x/L}) \right]. \quad (71)$$

The final result for I_ζ corresponds to the correlation function B_ζ given by Eq. (49), with $\sigma_\zeta^2 = B_\zeta(0) = \pi_0/M\pi_1$. Equation (70) provides a formula for the coherence function of a plane sound wave propagating in a turbulent atmosphere with intrinsic and global intermittency. It can actually be applied to local propagation paths such that $x \ll L$. Then, $e^{-x/L} \approx 1 - (x/L) + (x/L)^2/2$, and $I_\zeta \approx \sigma_\zeta^2 x^2$; that is, L ceases to affect the result. The main limitation of Eq. (70) is that integrals of the function ζ along the propagation path are assumed to have a Gaussian distribution.

Figure 7 compares coherence calculations from Eq. (70) with various combinations of intrinsic and global intermittency conditions. The turbulence parameters, based on the QW model, $a_N = 0.2$ m, $a_1 = 10$ m, $\phi/\mu = 0.0721$, and $\Delta T_1 = 0.866$ K. The path length is $x = 1$ km, the frequency 680 Hz (wavelength 0.5 m), and $L = 500$ m. The case with no intermittency ($\nu = 0$ and $\sigma_\zeta^2 = 0$) has the lowest coherence for all separations r. Intrinsic intermittency alone ($\nu = 1/6$ and $\sigma_\zeta^2 = 0$) increases the coherence for small separations ($r \lesssim a_1$), whereas global intermittency alone ($\nu = 0$ and $\sigma_\zeta^2 = 1/4$) increases the coherence for large separations. The combined effect ($\nu = 1/6$ and $\sigma_\zeta^2 = 1/4$) is an overall increase in coherence; it is nearly doubled for large separations.

Figure 8 shows the effect of changing the length scales a_1 and L. For each of the curves, $\nu = 1/6$ and $\sigma_\zeta^2 = 1/4$. One of the curves is for $a_1 = 10$ m and $L = 500$ m, as in Fig. 7. When a_1 is increased to 20 m, coherence increases for small separations but decreases for large ones. Increasing L to 2000 m, on the other hand, increases the coherence for all separations.

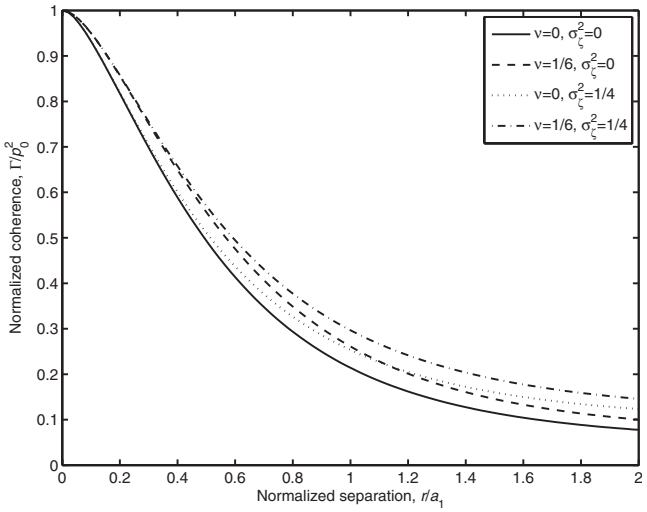

FIG. 7. Normalized coherence function vs the normalized sensor separation r/a_1 for different values of intrinsic intermittency (ν) and global intermittency σ_ζ^2. The correlation length of global intermittency $L=1$ km and the propagation path length is $x=5$ km.

C. Simulation results

In this subsection, the effects of intrinsic and global intermittency on the theoretical coherence function $\overline{\Gamma}(x,r)$ are studied with simulated random QW fields. The acoustic phases are calculated by numerically integrating Eq. (52) with the trapezoidal method. The use of geometric acoustics greatly simplifies the simulations and is justifiable for the reasons discussed in Sec. II B 2. (Simulations of random scattering by QWs, based on a finite-difference method, are described in Ref. 37. These do not involve the geometric approximation but are far more computationally intensive.) The simulations are for essentially the same situation in Figs. 7 and 8, although with intrinsic intermittency ($\nu=1/6$) always present. There are 362 QW size classes, and buffer regions were used around the edges as described in Sec. II A. Varying global intermittency conditions are considered:

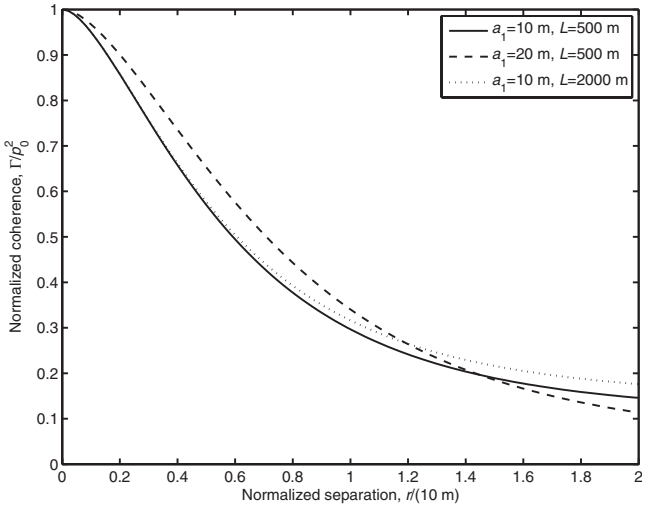

FIG. 8. Normalized coherence function vs sensor separation for different values of the outer scale a_1 and the correlation length of global intermittency L. All calculations include both intrinsic and global intermittency.

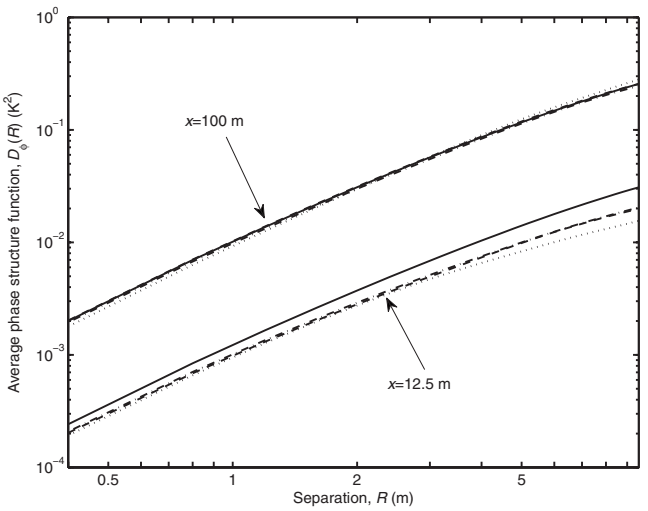

FIG. 9. Average phase structure function $\overline{D}_\phi(x,r)$ at distances $x=12.5$ m and $x=100$ m from the source, as a function of transverse separation between the observation points. The outer scale is 10 m and the correlation length of global intermittency is 500 m. The solid line is a theoretical prediction. The other lines are simulation data: Dashed is without global intermittency, dash dotted is moderate global intermittency, and dotted line is strong global intermittency.

none; $M=4$, $\pi_1=0.5$, and $L=500$ m; and $M=1$, $\pi_1=0.25$, and $L=500$ m. For the second of these cases, $\sigma_\zeta^2=1/4$. We designate this case *moderate* global intermittency. The third case, for which $\sigma_\zeta^2=3$, is designated *strong* global intermittency. All statistics were determined from 1024 random realizations.

Figures 9 and 10 show results for the average phase structure function, $\overline{D}_\phi(x,r)$, and average coherence, $\overline{\Gamma}(x,r)$, for propagation distances $x=12.5$ m and $x=100$ m. At these distances, the discussion in Sec. III A regarding local propagation paths ($x \ll L$) applies. The simulated curves for $\overline{D}_\phi(x,r)$ (Fig. 9) are nearly independent of the global intermittency condition, as they should be, since $\langle C \rangle$ is the same for each case. Theoretical predictions based on Eq. (66) agree very well with the simulations at $x=100$ m, but are too high at $x=12.5$ m. The reason for this overprediction is that

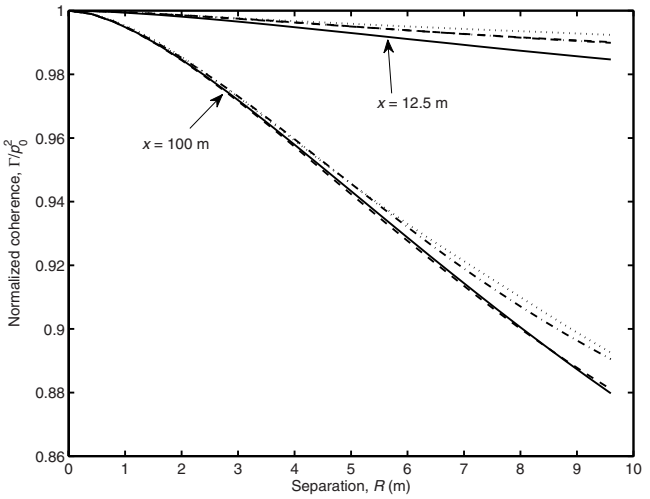

FIG. 10. (Color online) Normalized coherence function as a function of transverse separation. The curves correspond to the same cases in Fig. 9.

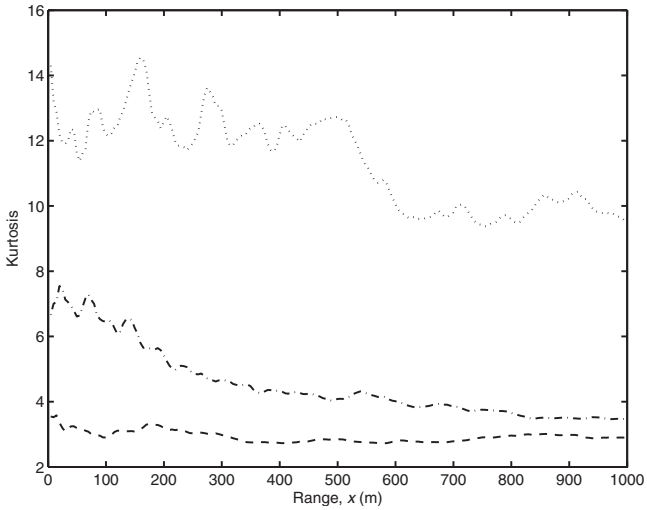

FIG. 11. Kurtosis of the phase difference fluctuations as a function of range x from the source. The separation between the observation points is 20 m. All curves are from an analysis of simulation data. The dashed line is without global intermittency, the dash-dotted line is moderate global intermittency, and the dotted line is strong global intermittency.

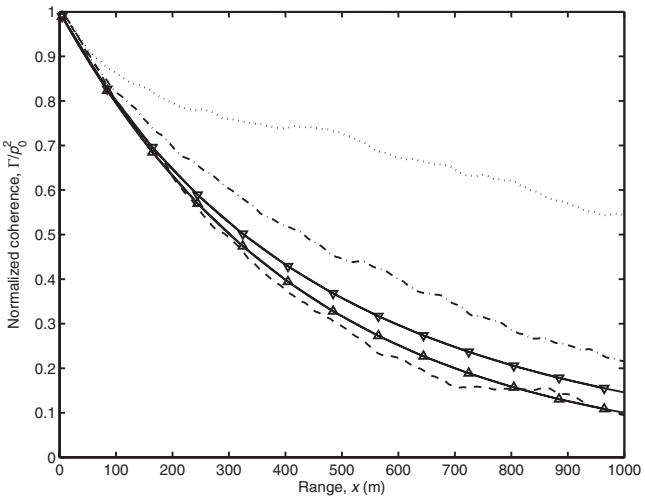

FIG. 12. Average coherence as a function of range x from the source. The separation between the observation points is 20 m. The solid lines are theoretical prediction without global intermittency (upward pointing triangles) and with moderate global intermittency (downward pointing triangles). The other lines are simulation data with the same interpretations as in Fig. 11.

$x \sim a_1$ at this distance, which means that the approximation $x \gg a_1$ inherent to Eqs. (57) and (62) is inapplicable. As might be expected, disagreement between the simulated average coherence at $x=12.5$ m and predictions based on the Gaussian approximation, Eq. (70) (Fig. 10), also results. Only one prediction from Eq. (70), corresponding to no global intermittency, is actually shown in Fig. 10 for each distance. This is because the Gaussian predictions are nearly independent of the global intermittency characteristics at these short distances. A particularly significant feature of Fig. 10 is the disagreement between the prediction and simulations at $x=100$ m when global intermittency is present, but not when global intermittency is absent. Since the average phase structure functions *are* correctly predicted (Fig. 9) in all cases, the assumption of Gaussian statistics upon which Eq. (70) is based must be at issue.

The significance of the non-Gaussian nature of the global intermittency is made clearer by Fig. 11, which shows the kurtosis of the phase differences, $[\phi(x,0)-\phi(x,r)]$ for $r=20$ m, as a function of range. The kurtosis for the case lacking global intermittency is nearly 3 at all ranges, as expected. For moderate intermittency, the kurtosis decays from 7 near the source to about 3.5 at $x=1$ km. For the strong intermittency, the kurtosis starts near 13 and remains quite high, around 10, at $x=1$ km. One would expect such strong non-Gaussianity to affect the average coherence and, indeed, as shown in Fig. 12, this is the case. The theoretical prediction and simulation without global intermittency are in good agreement. For moderate global intermittency, the simulated average coherence becomes somewhat higher than the prediction at distances $x>100$ m. No prediction is shown on the figure for strong global intermittency, because the prediction diverged in this case. The simulated coherence is dramatically raised by the strong global intermittency: It is about 0.55 at 1 km versus 0.1 without global intermittency. When there is such strong intermittency, the coherence is dominated by the many cases in which there is little turbulence along the propagation path.

IV. CONCLUSION

In this paper, a QW model of temperature fluctuations with both intrinsic and global intermittency was developed. Intrinsic intermittency was modeled by allowing the packing fraction to decrease with eddy size. Formulas for the 3D spectrum, variance, and kurtosis of temperature fluctuations were subsequently derived. It was shown that increasing the parameter ν, which characterizes the degree of intrinsic intermittency, results in decreasing variance, but increasing kurtosis, of temperature fluctuations. The increase in ν also leads to steepening of the inertial-subrange spectrum beyond the familiar $-11/3$ power law.

To introduce global intermittency into the QW model, the overall turbulence volume was partitioned into subvolumes in which intrinsic intermittency of the temperature fluctuations occurs as described above. Then, global intermittency was modeled by allowing the temperature amplitudes ΔT_1 of the largest QWs (eddies) to change randomly from one subvolume to another according to one or more superimposed Markov processes.

The developed statistical framework for describing intrinsic and global intermittency was then used as the basis for a theory of the coherence of a plane sound wave propagating through intermittent temperature fluctuations. Calculations based on this theory show that intrinsic and global intermittency both increase the average coherence. Simulations suggest that when global intermittency is very strong, such as might occur in stably stratified, night-time conditions, signal phase fluctuations become highly non-Gaussian and the coherence is dominated by episodes with little turbulence. This finding is important, e.g., for the performance of modern acoustic beam forming arrays, and should be examined experimentally. It would also be valuable to find analytical predictions for coherence in non-Gaussian conditions.

The QW model of temperature fluctuations with intrinsic and global intermittency is applicable with appropriate parameter adjustments to other intermittent scalar inhomogeneities, such as contaminants in the atmosphere and density fluctuations of geological heterogeneities within Earth, and can also be applied to other types of wave propagation, such as seismic and electromagnetic.

ACKNOWLEDGMENTS

This work was supported by U.S. Army In-House Laboratory Research Initiative (ILIR) and by U.S. Army Research Office Grant No. W911NF-06-1-0007. We thank J. C. Wyngaard and J. G. Brasseur (Pennsylvania State University) for many insightful discussions. We dedicate this manuscript to the memory of Dr. Steven Clifford and his many outstanding contributions to wave propagation in random media.

APPENDIX: SOLUTION FOR THE INTEGRAL *W*

A solution for the integral equation (64) is derived in this appendix. We begin by defining

$$I(y,s,a) = \int_0^\infty \xi^{-2a+1}\gamma(a,\xi^2 s^2)J_0(\xi y)d\xi. \tag{A1}$$

Then, Eq. (64) becomes

$$W(y,s) = (\pi^2/2)[I(0,s,a) - I(y,s,a)] \tag{A2}$$

with $a=11/6+\nu/2$.

We now determine the integral $I(y,s,a)$. First, we use Eq. (6.5.12) from Ref. 48 to write the incomplete gamma function as a confluent hypergeometric function. This gives

$$I(y,s,a) = a^{-1}s^{2a}\int_0^\infty \xi {}_1F_1(a;1+a;-\xi^2 s^2)J_0(\xi y)d\xi.$$

This integral can be solved with Eq. (7.663.6) from Ref. 49, which reads (with $\nu=0$)

$$\int_0^\infty x\,{}_1F_1(a;b;-\lambda x^2)J_0(xy)dx = \frac{2^{1-a}\Gamma(b)}{\Gamma(a)\lambda^{a/2}}y^{a-2}e^{-y^2/8\lambda}W_{a/2-b+1,a/2-1/2}\left(\frac{y^2}{4\lambda}\right). \tag{A3}$$

Here, $W_{k,\mu}$ is the Whittaker function. Setting $b=1+a$ and $\lambda=s^2$, we find

$$I(y,s,a) = 2^{1-a}s^a y^{a-2}e^{-y^2/8s^2}W_{-a/2,a/2-1/2}\left(\frac{y^2}{4s^2}\right). \tag{A4}$$

We can use Eq. (13.1.33) in Ref. 48 to rewrite this as

$$I(y,s,a) = \frac{1}{2}\left(\frac{y^2}{4}\right)^{a-1}e^{-y^2/4s^2}U\left(a,a,\frac{y^2}{4s^2}\right), \tag{A5}$$

where U is Kummer's confluent hypergeometric function. Finally, we use Eq. (13.6.28) in Ref. 48 to recast this result with an incomplete gamma function as follows:

$$I(y,s,a) = \frac{1}{2}\left(\frac{y^2}{4}\right)^{a-1}\Gamma\left(1-a,\frac{y^2}{4s^2}\right). \tag{A6}$$

A practical problem with this result for $I(y,s,a)$ is that routines for incomplete gamma functions in many numerical libraries do not allow negative arguments. In our case, without intermittency ($\nu=0$), we have $1-a=-5/6$. However, $\Gamma(a',x)$ [unlike $\gamma(a',x)$] is still a convergent function even when $a'<0$. This problem can be avoided by using the recursion relationship

$$\Gamma(a'+1,x) = a'\Gamma(a',x) + x^{a'}e^{-x}. \tag{A7}$$

Applying this recursion formula twice, we find

$$I(y,s,a) = \frac{s^{2(a-1)}}{2(a-1)}\left[\left(1-\frac{1}{a-2}\frac{y^2}{4s^2}\right)e^{-y^2/4s^2} + \frac{1}{a-2}\left(\frac{y^2}{4s^2}\right)^{a-1}\Gamma\left(3-a,\frac{y^2}{4s^2}\right)\right]. \tag{A8}$$

The argument to the incomplete gamma function is now positive. We also see that in the limit $y/s\to 0$,

$$I(0,s,a) = \frac{s^{2(a-1)}}{2(a-1)}. \tag{A9}$$

Finally, we have

$$W(y,s) = \frac{\pi^2 s^{2(a-1)}}{4(a-1)}\left[1-\left(1-\frac{1}{a-2}\frac{y^2}{4s^2}\right)e^{-y^2/4s^2} - \frac{1}{a-2}\left(\frac{y^2}{4s^2}\right)^{a-1}\Gamma\left(3-a,\frac{y^2}{4s^2}\right)\right]. \tag{A10}$$

For small arguments, $\Gamma(a,z)=\Gamma(a)-\gamma(a,z)\simeq\Gamma(a)-z^a/a$. Hence, for small y/s,

$$W(y,s) \simeq \frac{\pi^2 s^{2(a-1)}}{4(a-1)}\left\{1-\left(1-\frac{1}{a-2}\frac{y^2}{4s^2}\right)e^{-y^2/4s^2} - \frac{1}{a-2}\left(\frac{y^2}{4s^2}\right)^{a-1}\left[\Gamma(3-a)-\frac{1}{3-a}\left(\frac{y^2}{4s^2}\right)^{3-a}\right]\right\}. \tag{A11}$$

For $a=11/6$, the term proportional to $\Gamma(3-a)$ is the leading order term, and we have

$$W(y,s) \simeq \frac{\pi^2\Gamma(1/6)}{20}\left(\frac{y}{2}\right)^{5/3}. \tag{A12}$$

[1] V. Mellert and B. Schwarz-Rohr, "Correlation and coherence measurements of a spherical wave traveling in the atmospheric boundary layer," in Proceedings of the Seventh International Symposium on Long Range Sound Propagation, Lyon, France (1996), pp. 391–405.
[2] S. L. Collier, V. E. Ostashev, and D. K. Wilson, "Maximum likelihood estimation of the angle of arrival for an acoustic wave propagating in atmospheric turbulence," in Proceedings of the 2006 Meeting of the Military Sensing Symposia (MSS), Specialty Group on Battlefield Acoustic and Seismic Sensing, Magnetic and Electric Field Sensors, Laurel, MD (2006).
[3] A. Ishimaru, *Wave Propagation and Scattering in Random Media* (Academic, New York, 1978).
[4] S. M. Rytov, Yu. A. Kravtsov, and V. I. Tatarskii, *Principles of Statistical Radio Physics. Part 4, Wave Propagation Through Random Media* (Springer, Berlin, 1989).
[5] L. A. Chernov, *Waves in Randomly-Inhomogeneous Media* (Nauka, Mos-

cow, 1975) (in Russian).
[6]V. E. Ostashev, *Acoustics in Moving Inhomogeneous Media* (E & FN SPON, London, 1997).
[7]V. E. Ostashev and D. K. Wilson, "Coherence function and mean field of plane and spherical sound waves propagating through inhomogeneous anisotropic turbulence," J. Acoust. Soc. Am. **115**, 497–506 (2004).
[8]V. E. Ostashev, I. P. Chunchuzov, and D. K. Wilson, "Sound propagation through and scattering by internal gravity waves in a stably stratified atmosphere," J. Acoust. Soc. Am. **118**, 3420–3429 (2005).
[9]A. N. Kolmogorov, "A refinement of previous hypotheses concerning the local structure of turbulence in a viscous incompressible fluid at high Reynolds number," J. Fluid Mech. **13**, 82–85 (1962).
[10]A. M. Oboukhov, "Some specific features of atmospheric turbulence," J. Fluid Mech. **13**, 77–81 (1962).
[11]L. Mahrt, "Intermittency of atmospheric turbulence," J. Atmos. Sci. **46**, 79–95 (1989).
[12]U. Frisch, P.-L. Sulem, and M. Nelkin, "A simple dynamical model of intermittent fully developed turbulence," J. Fluid Mech. **87**, 719–736 (1978).
[13]A. Muschinski, R. G. Frehlich, and B. B. Balsley, "Small-scale and large-scale intermittency in the nocturnal boundary layer and the residual layer," J. Fluid Mech. **515**, 319–351 (2004).
[14]A. S. Gurvich and V. P. Kukharets, "The influence of intermittence of atmospheric turbulence on scattering of radio waves," Sov. J. Commun. Technol. Electron. **30**, 52–58 (1986).
[15]A. Muschinski, "Local and global statistics of clear-air Doppler radar signals," Radio Sci. **39**, RS1008 (2004).
[16]D. K. Wilson, J. C. Wyngard, and D. I. Havelock, "The effect of turbulent intermittency on scattering into an acoustic shadow zone," J. Acoust. Soc. Am. **99**, 3393–3400 (1996).
[17]D. K. Wilson, "Scattering of acoustic waves by intermittent temperature and velocity fluctuations," J. Acoust. Soc. Am. **101**, 2980–2982 (1997).
[18]D. E. Norris, D. K. Wilson, and D. W. Thomson, "Atmospheric scattering for varying degrees of saturation and turbulent intermittency," J. Acoust. Soc. Am. **109**, 1871–1880 (2001).
[19]V. E. Ostashev and D. K. Wilson, "Line-of-sight sound propagation through intermittent atmospheric turbulence," in Proceedings of the Ninth International Congress on Sound and Vibration, Orlando, FL (2002).
[20]A. S. Gurvich and A. M. Yaglom, "Breakdown of eddies and probability distributions for small-scale turbulence," Phys. Fluids **10**, 59–65 (1965).
[21]V. I. Tatarskii and V. U. Zavorotnyi, "Wave propagation in random media with fluctuating turbulent parameters," J. Opt. Soc. Am. A **2**, 2069–2076 (1985).
[22]H. G. E. Hentschel and I. Procaccia, "Passive scalar fluctuatations in intermittent turbulence with applications to wave propagation," Phys. Rev. A **28**, 417–426 (1983).
[23]R. Frehlich, "Laser scintillation measurements of the temperature spectrum in the atmospheric surface layer," J. Atmos. Sci. **49**, 1494–1509 (1992).
[24]R. Frehlich, "Effects of global intermittency on laser propagation in the atmosphere," Appl. Opt. **33**, 5764–5769 (1994).
[25]J. Gozani, "Effect of the intermittent atmosphere on laser scintillations," Opt. Lett. **24**, 436–438 (1999).
[26]J. Gozani, "Clarifying the concepts of wave propagation through intermittent media," Opt. Lett. **24**, 108–110 (1999).
[27]I. V. Petenko and E. A. Shurygin, "A two-regime model for the probability density function of the temperature structure parameter in the convective boundary layer," Boundary-Layer Meteorol. **93**, 381–394 (1999).
[28]G. H. Goedecke, V. E. Ostashev, D. K. Wilson, and H. J. Auvermann, "Quasi-wavelet model of von Kármán spectrum of turbulent velocity fluctuations," Boundary-Layer Meteorol. **112**, 33–56 (2004).
[29]G. H. Goedecke and H. J. Auvermann, "Acoustic scattering by atmospheric turbules," J. Acoust. Soc. Am. **102**, 759–771 (1997).
[30]G. H. Goedecke, D. K. Wilson, and V. E. Ostashev, "Quasi-wavelet models of turbulent temperature fluctuations," Boundary-Layer Meteorol. **120**, 1–23 (2006).
[31]G. H. Goedecke, V. E. Ostashev, and D. K. Wilson, "Quasi-wavelet models of turbulent temperature and shear-driven velocity fluctuations," in Proceedings of the 11th International Symposium on Long Range Sound Propagation, Fairlee, VT (2004), pp. 225–239.
[32]D. K. Wilson, G. H. Goedecke, and V. E. Ostashev, "Quasi-wavelet formulations of turbulence with intermittency and correlated field properties," in Proceedings of AMS-BLT Conference (2006).
[33]D. A. De Wolf, "A random motion model of fluctuations in a nearly transparent medium," Radio Sci. **18**, 138–142 (1983).
[34]W. E. McBride, H. E. Bass, R. Raspet, and K. E. Gilbert, "Scattering of sound by atmospheric turbulence: Predictions in a refractive shadow zone," J. Acoust. Soc. Am. **91**, 1336–1340 (1992).
[35]G. H. Goedecke, R. C. Wood, H. J. Auvermann, V. E. Ostashev, D. Havelock, and C. Ting, "Spectral broadening of sound scattered by advecting atmospheric turbulence," J. Acoust. Soc. Am. **109**, 1923–1934 (2001).
[36]D. K. Wilson, V. E. Ostashev, G. H. Goedecke, and H. J. Auvermann, "Quasi-wavelet calculations of sound scattering behind barriers," Appl. Acoust. **65**, 605–627 (2004).
[37]N. P. Symons, D. F. Aldridge, D. H. Marlin, D. K. Wilson, E. G. Patton, P. P. Sullivan, S. L. Collier, V. E. Ostashev, and D. P. Drob, "3D staggered-grid finite-difference simulation of sound refraction and scattering in moving media," in Proceedings of the 11th International Symposium on Long Range Sound Propagation, Fairlee, VT (2004), pp. 481–499.
[38]H. Sato and M. C. Fehler, *Seismic Wave Propagation and Scattering in the Heterogeneous Earth* (Springer, New York, 1998).
[39]S. Lovejoy and B. B. Mandelbrot, "Fractal properties of rain, and a fractal model," Tellus, Ser. A **37A**, 209–232 (1985).
[40]The simplest distribution for the $\tau^{\alpha n}$ is to set them to ± 1 with equal probability. Alternatively, they could be specified with a unit-variance Gaussian distribution. The distinction becomes important when discussing modeling field statistics higher than second order.
[41]F. Schmitt, S. Vannitsem, and A. Barbosa, "Modeling of rainfall time series using two-state renewal processes and multifractals," J. Geophys. Res. **103**, 23181–23193 (1998).
[42]S. Lovejoy and D. Scherzer, "Scale invariance, symmetries, fractals, and stochastic simulations of atmospheric phenomena," Bull. Am. Meteorol. Soc. **67**, 21–32 (1986).
[43]C. R. Chu, M. B. Parlange, G. G. Katul, and J. D. Albertson, "Probability density functions of turbulent velocity and temperature in the atmospheric surface layer," Water Resour. Res. **32**, 1681–1688 (1996).
[44]M. A. Jiménez and J. Cuxart, "Study of the probability density functions from a large-eddy simulation for a stably stratified boundary layer," Boundary-Layer Meteorol. **118**, 401–420 (2006).
[45]This formula is based on Eq. (41) in Ref. 30 [see Eq. (41) from that reference]. The primary difference is the appearance of the factor K_t, which allows various distributions to be used for the $\tau^{\alpha n}$. The presence of this factor can be readily understood from the discussion leading up to Eq. (38) in Ref. 30 [see Eq. (41) from that reference]. Multiplication of the first term on the right side of Eq. (38) extends that equation to any distribution for the $\tau^{\alpha n}$ having a unit variance. When this extension is carried through the subsequent derivation, the modification to Eq. (41) results.
[46]R. A. Antonia, A. J. Chambers, and E. F. Bradley, "Relationships between structure functions and temperature ramps in the atmospheric surface layer," Boundary-Layer Meteorol. **23**, 395–403 (1982).
[47]D. S. Wilks, *Statistical Methods in the Atmospheric Sciences* (Academic, Oxford, 2006).
[48]*Handbook of Mathematical Functions*, edited by M. Abramowitz and I. A. Stegun (Dover, San Francisco, CA, 1965).
[49]I. S. Gradshteyn and I. M. Ryzhik, *Table of Integrals, Series, and Products* (Academic, San Diego, CA, 1994).